Am J Cancer Res 2016;6(8):1799-1811
www.ajcr.us /ISSN:2156-6976/ajcr0032587

Original Article

Prognostic significance of *MST1R* dysregulation in renal cell tumors

Ana S Pires-Luís[1,2], Márcia Vieira-Coimbra[1,2], Maria João Ferreira[1], João Ramalho-Carvalho[1], Pedro Costa-Pinheiro[1], Luís Antunes[3], Paula C Dias[2], Francisco Lobo[4], Jorge Oliveira[4], Inês Graça[1], Rui Henrique[1,2,5], Carmen Jerónimo[1,5]

[1]Cancer Biology and Epigenetics Group, Research Center of The Portuguese Oncology Institute of Porto, Porto, Portugal; Departments of [2]Pathology, [3]Epidemiology, [4]Urology - Portuguese Oncology Institute of Porto, Porto, Portugal; [5]Department of Pathology and Molecular Immunology, Institute of Biomedical Sciences Abel Salazar (ICBAS), University of Porto, Porto, Portugal

Received May 22, 2016; Accepted May 29, 2016; Epub August 1, 2016; Published August 15, 2016

Abstract: Macrophage stimulating 1 receptor (*MST1R*) is a C-MET proto-oncogene family receptor tyrosine kinase. Promoter methylation patterns determine transcription of *MST1R* variants as hypermethylation of a region upstream of transcription start site (TSS) is associated with lack of MST1R long transcript ($MST1R_{long}$) and expression of a short transcript with oncogenic potential. Thus, we aimed to investigate *MST1R* variant transcript regulation in renal cell tumors (RCT) and assess their prognostic potential. We found, in a series of 120 RCT comprising the four main subtypes (clear cell, papillary and chromophobe renal cell carcinoma, and oncocytoma), that higher methylation levels close to TSS were associated with total *MST1R* expression levels ($MST1R_{total}$) in primary tumors (p=0.049) and renal cancer cell lines. After demethylating treatment, $MST1R_{long}/MST1R_{total}$ ratio increased, as expected, in two renal cell carcinoma cell lines tested. However, in primary tumors with hypermethylation upstream of TSS, a decrease in $MST1R_{long}/MST1R_{total}$ ratio was not detected, although higher expression ratio of nuclear factor-κB was apparent. Furthermore, survival analysis demonstrated that $MST1R_{long}/MST1R_{total}$ ratio was independently associated with shorter disease-specific and disease-free survival, whereas $MST1R_{total}$ expression associated with shorter disease-specific survival. In conclusion, although promoter methylation patterns seem to determine *MST1R* global transcription regulation in renal cell carcinoma, other mechanisms might contribute to deregulate *MST1R* variant expression in RCT. Nevertheless, $MST1R_{total}$ expression and $MST1R_{long}/MST1R_{total}$ ratio modulate the biological and clinical aggressiveness of renal cell carcinoma, as depicted by its prognostic significance, a finding that requires validation in a larger independent series.

Keywords: Renal cell tumors, *MST1R*, *RON*, *MST1R* promoter methylation, MST1R expression, epigenetics

Introduction

The macrophage stimulating 1 receptor (*MST1R*), also known as RON (recepteur d'origine nantais), is a C-MET proto-oncogene family receptor tyrosine kinase [1]. Both *MST1R/RON* and its ligand, macrophage-stimulating protein (MSP) [2], are mapped at chromosome 3p21 [1, 3], and MSP binding triggers *MST1R* dimerization and subsequent activation [4]. This leads to downstream signaling activation of RAS-MAPK and PI-3K-AKT pathways [4], determining increased proliferation, survival and invasion [5], epithelial to mesenchymal transition (EMT) [6] and chemoresistance [7]. Since the nomenclature used for *MST1R/RON* varies in different references, we will follow the designation used in the original study whenever we consider that it prevents further confusion, but otherwise we will use *MST1R*.

MST1R is constitutively transcribed in epithelial cells, macrophages, osteoclasts and hematopoietic cells [8-12], and its signaling was reported to be altered in several human cancers, including those of the breast [13], lung [14], liver [15], ovary [16], colon [17], bladder [18] and nasopharynx [19].

In addition to ligand-induced dimerization, *MST1R* activation may be accomplished by

receptor overexpression, kinase domain activating mutations and generation of constitutively active *MST1R* variants [4, 20]. Most of these variants originate from full-length *MST1R* (*flRON*) alternative mRNA splicing (*RONΔ170*, *RONΔ165*, *RONΔ160*, *RONΔ155*), but may also be generated from protein truncation (*RONΔ110, RONΔ75*) and alternative transcription start site (short-form RON, *sfRON*, or *RONΔ55*) [21]. Some of these variants are constitutively active and thought to be oncogenic, including *RONΔ165*, *RONΔ160*, *RONΔ155* and *RONΔ110* [21].

Concerning alternative transcription start site, two *MST1R* transcripts are often found in both normal and neoplastic cells, named full-length *RON* (*flRON*) and short-form *RON* (*sfRON*) [22, 23]. Whereas *flRON* transcription is initiated through a classical promoter upstream transcription start site (TSS) and it is enhanced by hypoxia-inducible factor 1α (*HIF-1α*) [24], early growth response-1 (*Egr-1*) [25] and nuclear factor-κB (*NF-κB*) [25] in cancer cells, *sfRON* transcription is initiated at the codon that encodes for Met913, using an alternative intragenic promoter located between introns 8 and 10 [12, 22]. Scarce data is available on alternative transcription start site regulation, but it has been reported that methylation pattern of MST1R promoter associates with differential *flRON* and *sfRON* expression: hypermethylation at an area upstream of *MST1R* promoter, named 'island 1', was associated with absence of *flRON* and the presence of *sfRON* expression, whereas 'island 1' low or absent methylation was associated with concomitant *flRON* and *sfRON* expression [22]. It was also suggested that *sfRON* endogenous activity might be influenced by *flRON* expression, since a protein complex that is promptly degraded is formed when both *sfRON* and *flRON* are co-expressed [22]. Hence, when 'island 1' is hypermethyalted, *MST1R* homeostasis is shifted towards *flRON* null or low expression levels, and increased *sfRON* expression and activity. *sfRON* protein is constitutively active and its overexpression has been associated with an aggressive tumor phenotype: cancer cells grow faster, lose epithelial morphology, cease to form cell aggregates and become motile [23], features that promote local invasion and metastatic spread.

Despite *MST1R* signaling was found to be deregulated in several neoplasms [13-19, 22, 23], few studies have focused on *MST1R* promoter methylation [22], particularly in renal cell tumors (RCT). We have previously reported that *MST1R* promoter hypermethylation in renal cell tumors (RCT) was a sensitive and specific biomarker for clear cell renal cell carcinoma [26], and the 307 renal tumors available in the "Catalogue of somatic mutations in cancer" (COSMIC) dataset (cancer.sanger.ac.uk) were reported as highly methylated [27]. RCTs, a clinical, morphological, genetically and epigenetically heterogeneous group of tumors, comprise both benign [e.g., oncocytoma (RO)], and malignant [e.g., clear cell renal cell carcinoma (ccRCC), papillary RCC (pRCC) and chromophobe RCC (chRCC)] neoplasms, among which ccRCC is the most frequent (75%) and aggressive subtype, followed by pRCC (10%), and then chRCC (5%), the least aggressive subtype that rarely metastasizes [28, 29]. Although *MST1R* protein expression has been previously investigated in RCTs, it mainly focused on chRCC and RO [30, 31], and, thus, studies on *MST1R* mRNA expression deregulation through promoter methylation, as well as its biological and clinical impact are lacking. Thus, we aimed to characterize *MST1R* promoter methylation in RCT to investigate whether altered patterns might associate with different transcript variant expression in RCT primary tumors and cell lines, and how it might impact on tumor aggressiveness.

Material and methods

Patients and sample collection

Fresh-frozen tissue was prospectively collected, after informed consent, from 130 nephrectomy specimens at the Portuguese Oncology Institute - Porto (Portugal) between 2003 and 2007, comprising samples from ccRCC, pRCC, chRCC and oncocytoma (30 of each), and 10 morphologically normal kidney (cortical) tissue (from patients with upper urinary tract neoplasia not invading the renal parenchyma). Tissue samples were snap-frozen immediately after surgery, stored at -80°C and later cut in a cryostat. An H&E slide was performed before and after the sections used for nucleic acid extraction, to ensure at least 70% of neoplastic cells in the tumor samples and negligible inflammation in morphologically normal kidney samples.

Routine assessment of tumor classification (WHO), grading (Fuhrman) and staging (TNM)

Table 1. Primer sequences, amplicon size, and annealing temperatures for *MST1R* [GenBank: NM_002447] bisulfite sequencing (BSP), quantitative methylation specific PCR (QMSP) and expression

Primer set	Sense primer sequence (5'-3')	Antisense primer sequence (5'-3')	Amplicon size (bp)	Location [bp upstream (up) or downstream (down) TSS]	Annealing temp (°C)
BSP					
MST1R_B_1	GTTATTGAGGGTGTTGTTATTAAGTG	ACCTAACCCAAACCCTCC	264	612 up to 348 up	60
MST1R_B_2	AGGTGAAGGTATAGGAGTTAGG	AAATTCCTATAAAACCCAAATC	272	417 up to 145 up	60
MST1R_B_3	GGTAGGGATTTTTTAGGGTTT	CACCATAACCTATACCAAACCTC	210	33 up to 177 down	60
QMSP					
$MST1R_{up}$	TTAAGGGTCGGAAGAGTC	ATACACTAACGCTTAACGCTC	128	540 up to 412 up	60
$MST1R_{TSS}$	AGCGTTAGTGTATAGCGGC	TAAACAACGATCCCGACA	169	270 up to 101 up	60
Expression					
$MST1R_{total}$	GGCTGAGGTCAAGGATGTGCT	GCCTTTGCCAATGACTCGGT	73	-	62
$MST1R_{long}$	CTCTGGGGACCAGGTTTTC	ATGAAATGCCATGCCCTTAG[a]	93	-	62
NF-κB	GCTTAGGAGGGAGAGCCCT	CTGCCATTCTGAAGCCGGG	86	-	61

[a]Primer sequence from [23].

was performed for all tumor cases in formalin-fixed paraffin-embedded tissue [29, 32]. Relevant clinical data was collected from clinical charts.

This study was approved by the Institutional Review Board (Comissão de Ética para a Saúde) of Portuguese Oncology Institute of Porto, Portugal (CES518/2010).

Cancer cell lines

Cell lines representative of ccRCC, two established from primary tumors (769-P, 786-O) and one from a metastatic site (Caki-1) were obtained from the American Type Culture Collection (Manassas, VA). All cell lines were cultured according to the manufacturer's specifications, with 10% fetal bovine serum (Gibco, Invitrogen, Carlsbad, CA) and antibiotics (100 units/mL penicillin G and 100 µg/mL streptomycin, Gibco), in a humidified atmosphere of 5% CO_2 at 37°C.

769-P and 786-O cancer cell lines were subjected to treatment with the demethylating drug 5-aza-2'deoxycytidine (1 µM for 72 h). In parallel, the same cell lines were cultured without treatment for 72 h and harvested before confluence. Demethylating treatment was conducted in triplicate for both cell lines.

Nucleic acid extraction

Genomic DNA from fresh-frozen samples and cell lines was extracted as previously described [33]. In brief, DNA was digested overnight with proteinase K (20 mg/mL) in the presence of 10% SDS at 55°C, and then extracted with phenolchloroform and precipitated with 100% ethanol.

RNA extraction was performed as previously reported [34] both for fresh-frozen tissues and cell lines. Briefly, TRIzol® reagent (Invitrogen™, Carlsbad, CA, USA) was used to suspend the samples, chloroform (Merk Millipore, Darmstadt, Germany) was added to the lysed cells, and total RNA was then purified using Ambion® PureLink RNA Mini Kit (Invitrogen™, Carlsbad, CA, USA), according to manufacturer's recommendations. RNA purity ratios and concentration were measured in a NanoDrop ND-1000 spectrophotometer (NanoDrop Technologies, Wilmington, DE, USA) and RNA quality was confirmed by electrophoresis.

Bisulfite modification and bisulfite sequencing

Bisulfite conversion of unmethylated cytosine residues to uracil, whereas methylated cytosine residues remain as such, was performed using the EZ DNA Methylation-Gold Kit (Zymo Research, Orange, CA, USA), according to manufacturer's instructions. The modified DNA was eluted in 60 mL of water and stored at -80°C.

Subsequently, *MST1R* [GenBank: NM_002447] promoter was subjected to direct bisulfite sequencing in 5 samples: 1 ccRCC, 1 pRCC, 1 chRCC, 1 RO and 1 normal kidney. Primers were specifically designed to amplify fragments containing the *MST1R* promoter CpG "island 1"

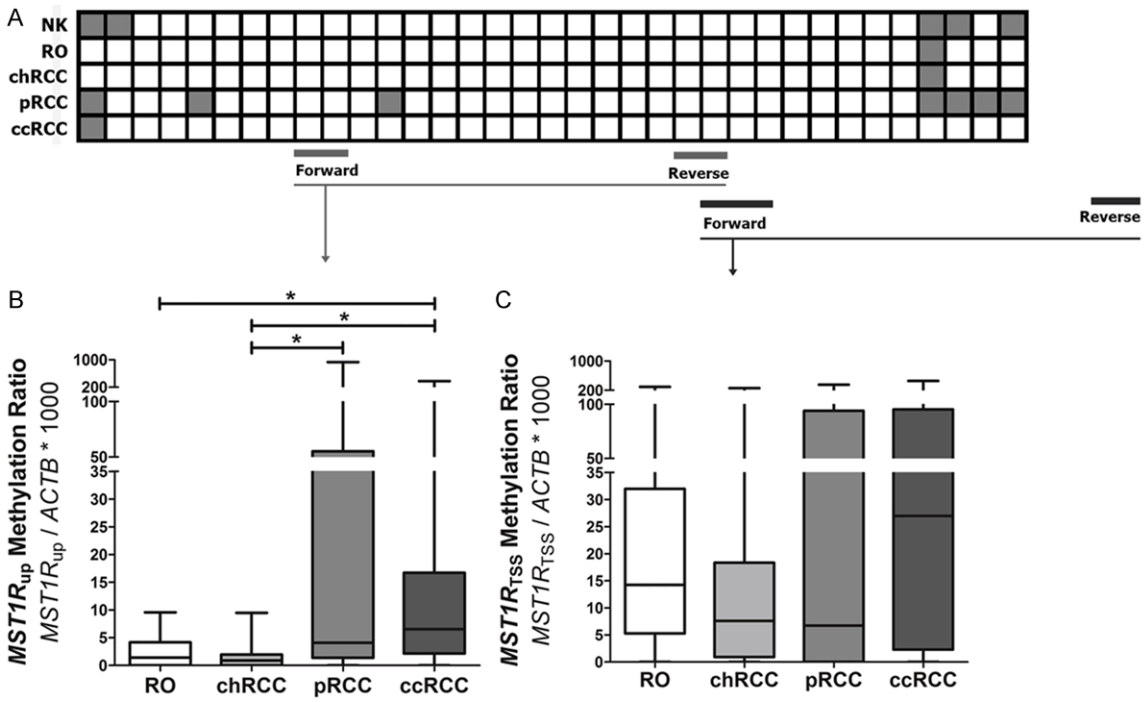

Figure 1. *MST1R* promoter methylation in renal cell tumors (RCT): bisulfite sequencing of *MST1R* promoter in 5 cases (A) and QMSP methylation levels in two distinct regions, one upstream TSS ($MST1R_{up}$) and another closer to TSS ($MST1R_{TSS}$), in 120 cases. White squares: CpG unmethylated; gray squares: CpG partially methylated. NK: normal kidney; RO: renal oncocytoma; chRCC: chromophobe renal cell carcinoma; pRCC: papillary renal cell carcinoma; ccRCC: clear cell renal cell carcinoma.

[22], using Methyl Primer Express v 1.0 (Applied Biosystems, Foster City, CA, USA). Primer sequences and location, amplicons, and annealing temperatures are listed in **Table 1**.

PCR reactions included a 94°C denaturation 10 min. step followed by 40 cycles at 94°C for 30 sec., annealing temperature for 30 sec., and 72°C for 30 sec. PCR products were loaded in a 2% agarose gel, stained with ethidium bromide and visualized under an ultraviolet transilluminator. Excess primer and nucleotides were removed by Illustra GFX PCR DNA and Gel Band Purification kit (GE Healthcare, USB Corporation, Cleveland, OH, USA) following manufacturer's protocol. The purified products were sequenced using the dGTP BigDye Terminator Cycle Sequencing ReadyReaction kit (Applied Biosystems, Foster City, CA, USA) in an ABI PRISM 310 Genetic Analyzer (Applied Biosystems, Foster City, CA, USA), and data were analyzed by Sequencer Version 4.2.2 software. The peak height of the cytosine signal and the sum of the cytosine and thymine peak height signals were compared to calculate the approximate amount of methylcytosine of each CpG site. CpG sites with ratios 0-0.20, 0.21-0.80, and 0.81-1.0 were considered unmethylated, partially methylated, and fully methylated, respectively, as previously described [33, 35].

Quantitative MSP

Quantitative methylation specific real-time polymerase chain reaction (QMSP) was performed in cell lines before and after demethylating treatment, and in all frozen tissue samples, after DNA bisulfite conversion.

Primers were designed to specifically amplify methylated bisulfite converted complementary sequences of *MST1R* promoter using Methyl Primer Express v 1.0 (Applied Biosystems, Foster City, CA, USA), enclosing the region previously described as *MST1R* promoter "island 1" [22], located upstream of TSS [26]. Two areas were amplified, one upstream "island 1" but still in the *MST1R* promoter CpG island, and another downstream, more close to TSS, named $MST1R_{up}$ and $MST1R_{TSS}$ respectively (**Figure 1**). Primer sequences and location are listed in **Table 1**. β-*actin* (*ACTB*) was used as

reference gene to normalize for DNA input in each sample.

For QMSP analysis, a reaction volume of 20 μL consisting of 10 μL of SYBR® Green PCR Master Mix (Applied Biosystems, Foster City, CA, USA), 7 μL of H_2O, 0.5 μL of forward primer, 0.5 μL of reverse primer and 2 μL of bisulfate-modified DNA, was run in an 7500 Real-time PCR system (Applied Biosystems, Foster City, CA, USA). Each sample was run in triplicate, a calibration curve was constructed with serial dilutions (1:5) of bisulfite converted universally methylated DNA at all CpGs (CpGenome Universal Methylated DNA; Millipore, Billerica, MA) to quantify the amount of fully methylated alleles in each reaction, and "no template controls" were included as a control for contamination. The amplification reaction was carried out at 95°C for 2 min followed by 45 cycles of 95°C for 15 s, and at annealing temperature (**Table 1**) for 1 min, followed by a melt curve.

Relative levels of methylated promoter DNA in each sample were determined by the ratio of the mean quantity obtained by QMSP analysis for each gene and the respective value of the internal reference gene (*ACTB*), multiplied by 1000 for easy tabulation (methylation level = target gene/reference gene × 1000).

Quantitative gene expression analysis

MST1R gene expression was evaluated in ccRCC cell lines before and after treatment when done, and in the 120 RCTs samples. For cell lines, 1 μg of total RNA was reversely transcribed using the High Capacity cDNA Reverse Transcription kit (Applied Biosystems®, Foster City, CA, USA) according to manufacturer instructions. For frozen tissue, 300 ng of total RNA was reversely transcribed and amplified using TransPlex® Whole Transcriptome Amplification Kit (Sigma-Aldrich®, St. Louis, MO, United States) purified with QIAquick PCR Purification Kit (QIAGEN, Germany). Total *MST1R* expression ($MST1R_{total}$) and long form *MST1R* expression ($MST1R_{long}$) was evaluated using custom primers designed respectively to a region common to all *MST1R* described transcripts and to a region specific of the long form transcript (**Table 1**), using a Light Cycler 480 Real-time PRC system (Roche, Basel, Switzerland), in a reaction volume of 10 μL consisting of 5 μL of KAPA SYBR FAST® qPCR Master Mix (Kapa Biosystems, Wilmington, MA, USA), 3.7 μL of H_2O, 0.15 μL of forward primer, 0.15 μL of reverse primer and 1 μL of cDNA.

Each sample was run in triplicate and the amount of cDNA was normalized to Glucuronidase beta (*GUSβ*) reference gene, as the ratio of the mean expression level obtained by QMSP analysis for each transcript and the respective value of the internal reference gene (*GUSβ*), multiplied by 1000 for easy tabulation. Each plate included multiple non-template controls and serial dilutions (1:5) of a cDNA Human Reference Total RNA (Agilent Technologies, La Jolla, CA, USA) to construct a standard curve.

NF-κB expression was evaluated in the 120 RCTs, as described above, using custom primers (**Table 1**).

Statistical analysis

Median and interquartile range of promoter methylation and expression levels were determined for cell lines and tumor samples. For tumor samples analysis and for each QMSP primer pair, each RCT sample was classified as "methylated" if the methylation level was higher than the highest value determined in the normal kidney samples ($MST1R_{up}$: 17.58; $MST1R_{TSS}$: 2.22), and as "not methylated" if the methylation level was lower than that value. $MST1R_{long/total}$ ratio was computed as the ratio $MST1R_{long}/MST1R_{total}$ x 100, after linear normalization of $MST1R_{total}$ relative expression [($MST1R_{total}$ value - $MST1R_{total}$ min)/($MST1R_{total}$ max - $MST1R_{total}$ min)] and $MST1R_{long}$ relative expression [($MST1R_{long}$ value - $MST1R_{long}$ min)/($MST1R_{long}$ max - $MST1R_{long}$ min)].

Non-parametric tests were used to ascertain the statistical significance of differences among groups of samples, namely Kruskal-Wallis ANOVA test (KW) for multiple comparisons and Mann-Whitney U test (MW) with Bonferroni's correction for pair-wise comparisons, as appropriate. Spearman's test was carried out to ascertain correlations between age and gene expression levels.

Prognostic significance of standard clinicopathological variables (histological subtype, pathological stage, Fuhrman grade, age, gender) and of $MST1R_{up}$ and $MST1R_{TSS}$ methylation level, $MST1R_{long/total}$ ratio, $MST1R_{total}$ and *NF-κB* expression levels, was assessed by constructing

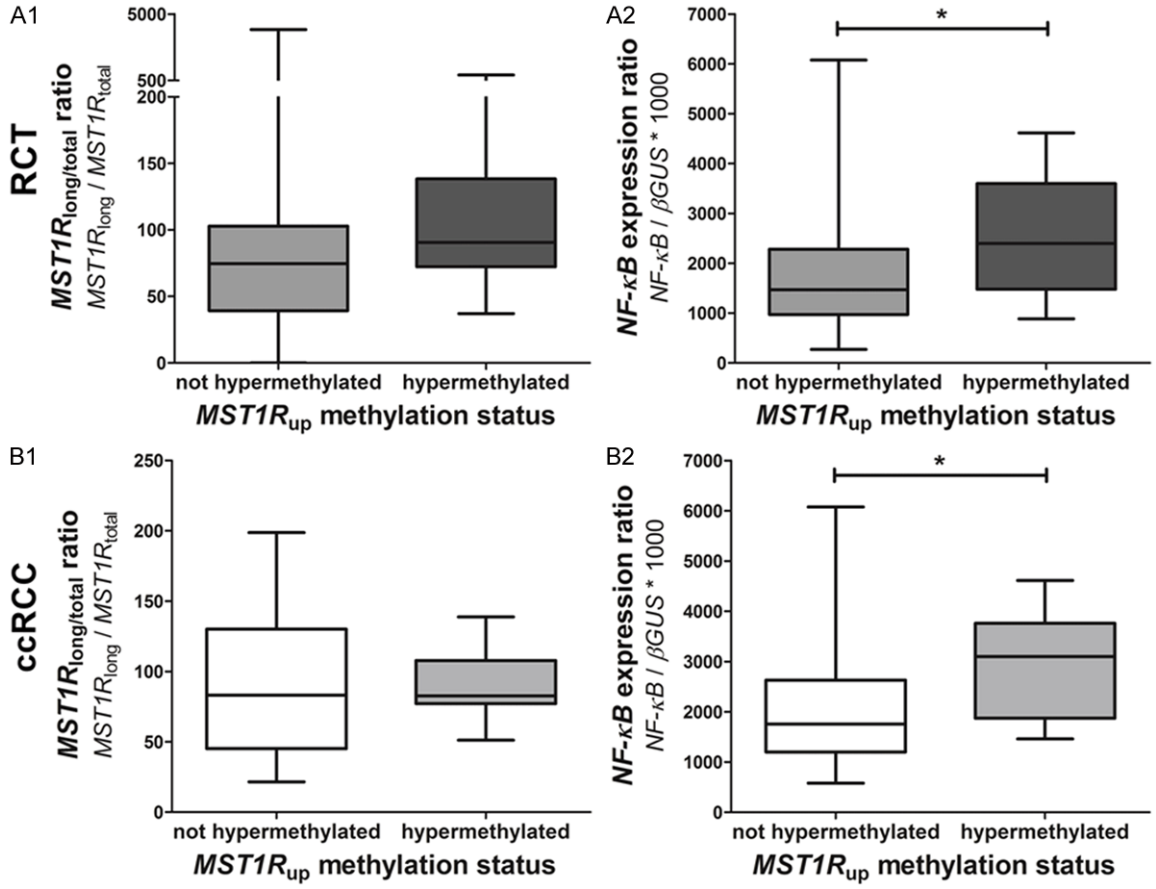

Figure 2. Expression levels in tumors hypermethylated or not at $MST1R_{up}$ (upstream area of *MST1R* promoter): $MST1R_{long/total}$ ratio in RCTs (n=120) (A1) and in ccRCC (n=30) (B1), and *NF-κB* expression ratio in RCTs (A2) and ccRCC (B2).

disease-specific and disease-free survival (defined, respectively, as the time between diagnosis and death for renal cell carcinoma, and the time between treatment and the first metastasis or local recurrence) curves using the Kaplan-Meier method, with log-rank test (univariable test). For this purpose, expression levels and ratio were classified as low or high using as cut-off the 75th percentile expression value of each gene/ratio. Multivariable survival analysis was conducted only for ccRCC and pRCC. The exclusion of chRCC from the analysis was due to the paucity of events (one patient presented progression/metastasis during follow-up and none has died from cancer). Age, stage and histological subtype were also included in the final Cox-regression model, both for disease-specific (DSS) and disease-free (DFS) survival.

Statistical significance was set at $p < 0.05$. Statistical analysis was performed using SPSS software for Windows, version 22.0 (IBM-SPSS Inc., Chicago, IL, USA), and graphs were built using GraphPad Prism 6.0 software for Windows (GraphPad Software Inc., La Jolla, CA, USA).

Results

MST1R promoter methylation is higher near TSS in renal cell tumors

The methylation pattern of *MST1R* promoter in RCTs was characterized by QMSP using two primer sets, one upstream TSS ($MST1R_{up}$) and another more close to TSS ($MST1R_{TSS}$). Globally, $MST1R_{TSS}$ methylation levels [median (range): 14 (0-458)] was higher than those of $MST1R_{up}$ [median (range): 2 (0-933)], and 74% of samples were hypermethylated at $MST1R_{TSS}$ (22 ccRCC, 20 pRCC, 22 chRCC and 25 oncocytomas) whereas only 10% of samples were hypermethylated at $MST1R_{up}$ (4 ccRCC and 8 pRCC).

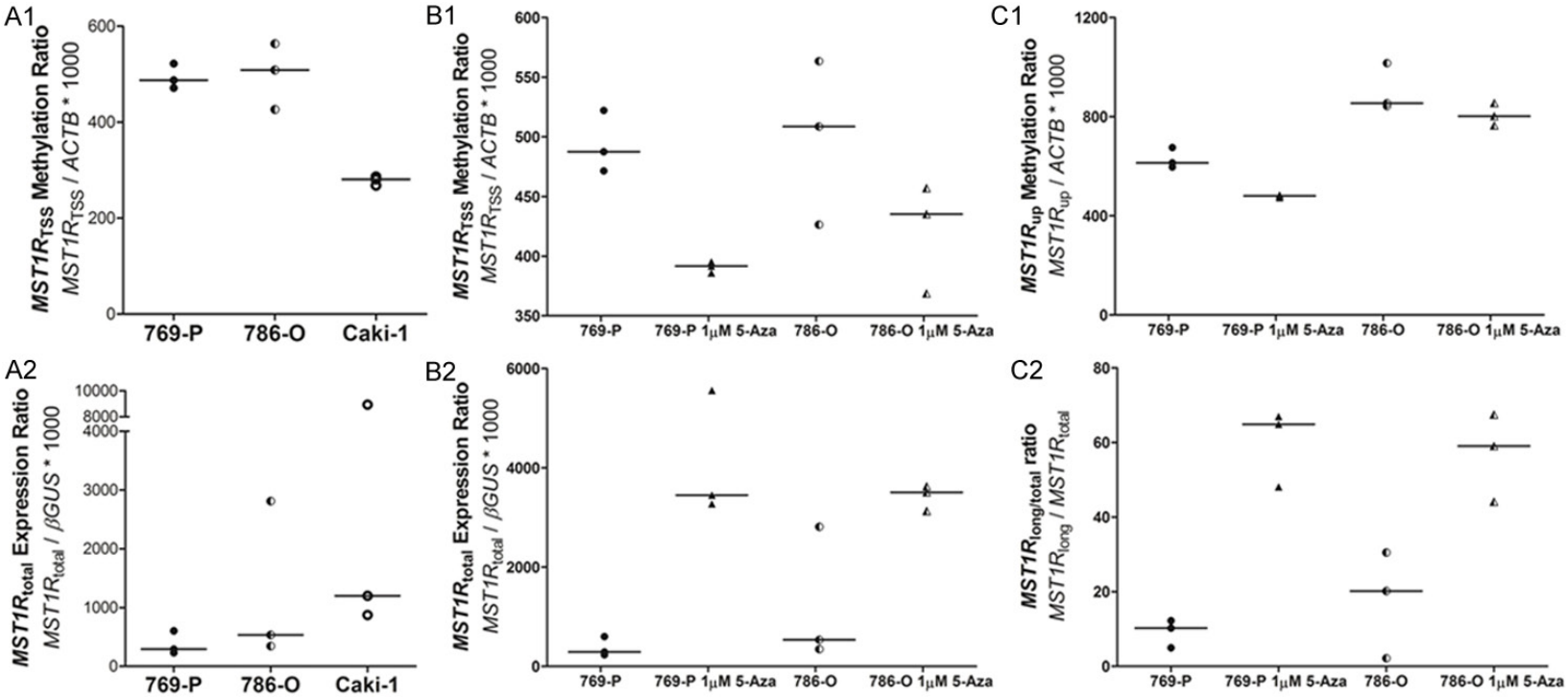

Figure 3. *MST1R* methylation and expression levels in ccRCC cell lines. A: $MST1R_{TSS}$ methylation level (A1) and $MST1R_{total}$ expression level (A2) in three cell lines. B: $MST1R_{TSS}$ methylation level (B1) and $MST1R_{total}$ expression level (B2) in 769-P and 786-O cell lines before and after demethylating treatment with 1 μM 5-aza-2'deoxycytidine for 72 h. C. $MST1R_{up}$ methylation level (C1) and $MST1R_{long/total}$ ratio (C2) in 769-P and 786-O cell lines before and after demethylating treatment with 1 μM 5-aza-2'deoxycytidine for 72 h.

Table 2. Clinical and pathological data of patients included in the present study

	Tumor	Normal
Number of patients, n	120	10
Age, median (range)	60 (29-83)	67.5 (20-83)
Gender, n (%)		
Male	73 (61)	7 (70.0)
Female	47 (39)	3 (30.0)
Histological subtype, n (%)		n.a.
Clear cell RCC	30 (25)	
Papillary RCC	30 (25)	
Chromophobe RCC	30 (25)	
Oncocytoma	30 (25)	
Pathological Stage, n (%)		n.a.
Stage I	47 (39)	
Stage II	19 (16)	
Stage III	21 (17.5)	
Stage IV	3 (2.5)	
n.a. (oncocytoma)	30 (25)	
Fuhrman grade, n (%)		n.a.
1	3 (2.5)	
2	28 (23)	
3	45 (37.5)	
4	14 (12)	
n.a.	30 (25)	

n.a.: not applicable.

This is in line with overall results of bisulfite sequencing in the 5 samples analyzed, which revealed rare methylated CpG in the $MST1R_{up}$ area, and an increase of methylated CpG dinucleotides near TSS (**Figure 1A**). Additionally, at $MST1R_{up}$, significantly higher methylation level were depicted for ccRCC and pRCC compared to chRCC, and for ccRCC compared to oncocytoma ($p<0.001$ for all) (**Figure 1B**). There were no statistically significant differences in $MST1R_{TSS}$ methylation levels among RCT subtypes ($p=0.291$) (**Figure 1C**).

NF-κB expression associates with $MST1R_{long/total}$ ratio in hypermethylated RCTs

RCTs with $MST1R_{TSS}$ hypermethylation showed a significantly lower $MST1R_{total}$ expression ratio ($p=0.049$), and RCTs with $MST1R_{up}$ hypermethylation displayed a trend for higher expression of $MST1R_{long/total}$, ($p=0.053$) (**Figure 2A**). Interestingly, a significantly higher expression of NF-κB ($p=0.013$) was also observed in these RCTs (**Figure 2B**).

When analyzing ccRCC and pRCC independently ($MST1R_{up}$ hypermethylation was not apparent in chRCC or oncocytomas), there were no differences in $MST1R_{long/total}$ in ccRCC with or without $MST1R_{up}$ hypermethylation ($p=0.756$) (**Figure 2C**), but ccRCC with $MST1R_{up}$ hypermethylation displayed a significantly higher NF-κB expression ($p=0.036$) (**Figure 2D**). No statistically significant differences were depicted for pRCC.

MST1R expression is regulated by promoter methylation pattern in ccRCC cell lines

MST1R promoter methylation levels more close to TSS ($MST1R_{TSS}$) and $MST1R_{total}$ expression was evaluated in 769-P, 786-0 and Caki-1 ccRCC cell lines. $MST1R_{total}$ expression was lowest in 769-P and 786-0 cells (**Figure 3A2**), which also displayed the highest $MST1R_{TSS}$ methylation levels (**Figure 3A1**), paralleling the observations in primary tumors. Demethylating treatment in those two cell lines restored $MST1R_{total}$ expression (**Figure 3B2**), mainly $MST1R_{long}$ (*flRON*) expression, which was apparent through a higher $MST1R_{long/total}$ ratio (**Figure 3C2**), and decreased $MST1R_{TSS}$ and $MST1R_{up}$ methylation levels (**Figure 3B1** and **C1**).

Clinical-pathological associations and survival analysis

Clinical and pathological features of the 120 patients included in this study are depicted in **Table 2**. The methylation levels of $MST1R_{up}$ and $MST1R_{TSS}$, as well as $MST1R_{total}$ expression level, $MST1R_{long/total}$ ratio and *NF-κB* expression level, were not associated with gender ($p=0.563$, $p=0.263$, $p=0.561$, $p=0.159$ and $p=0.576$, respectively), age ($p=0.352$, $p=0.979$, $p=0.676$, $p=0.119$ and $p=0.056$, respectively) or pathological stage ($p=0.661$, $p=0.908$, $p=0.132$, $p=0.579$ and $p=0.822$, respectively).

A significantly lower *NF-κB* expression level ($p<0.001$) was observed in oncocytomas compared to RCC, whereas for $MST1R_{up}$ and $MST1R_{TSS}$ methylation levels, $MST1R_{total}$ expression levels and $MST1R_{long/total}$ ratio, no significant differences were found.

During follow-up [median (range): 60 months (2-392 months)], 12 (13%) patients died from RCC and 17 (19%) developed metastatic disease. Among molecular parameters, only $MST1R_{total}$ expression levels associated with

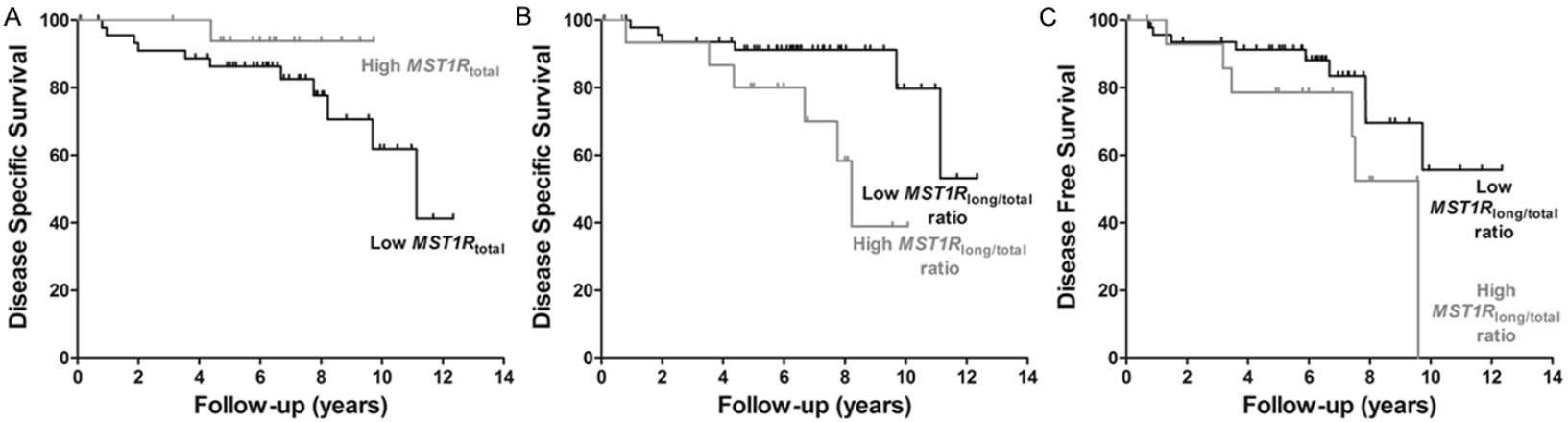

Figure 4. Kaplan-Meier analysis for disease-specific survival in 60 RCC patients, according to $MST1R_{total}$ expression level (A) and $MST1R_{long/total}$ ratio (B), and for disease-free survival in 60 RCC patients, according to $MST1R_{long/total}$ ratio (C). The results presented were categorized using third quartile (75^{th} percentile) value as cutoff.

Table 3. Prognostic value of pathological stage, histological subtype and *MST1R* expression in renal cell carcinomas, following multivariable analysis using Cox-regression model

Prognostic Factor	Multivariable Analysis		
	Hazard Ratio (HR)	95% CI for HR	Cox regression *p* value
Disease Specific Survival[a]			
- Stage III/Stage IV (*vs* Stage I/Stage II)	38	5.4-269	< 0.001
- pRCC (*vs* ccRCC)	22	3.1-157	0.002
- High $MST1R_{total}$ expression level (*vs* low $MST1R_{total}$ expression level)	10	1-96	0.046
- Stage III/Stage IV (*vs* Stage I/Stage II)	26	4.4-153	< 0.001
- pRCC (*vs* ccRCC)	14.6	2.2-99	0.006
- Low $MST1R_{long}/MST1R_{total}$ ratio (*vs* high $MST1R_{long}/MST1R_{total}$ ratio)	4.9	1.2-20	0.025
Disease Free Survival[b]			
- Stage III/Stage IV (*vs* Stage I/Stage II)	14	3.5-59	< 0.001
- Low $MST1R_{long}/MST1R_{total}$ ratio (*vs* high $MST1R_{long}/MST1R_{total}$ ratio)	3.2	1.1-9.5	0.038

Only ccRCC and pRCC were included due to insufficient events in chRCC. CI: Confidence Interval; ccRCC: clear cell renal cell carcinoma; pRCC: papillary renal cell carcinoma. [a]Adjusted for patient age. [b]Adjusted for patient age and histological subtype; $MST1R_{total}$ expression level did not attained statistical significance in multivariable analysis for disease free survival.

development of metastasis during follow-up (p=0.049). Patients with a low RCC $MST1R_{total}$ expression displayed shorter DSS, and those with high $MST1R_{long/total}$ ratio presented shorter DSS and DFS (**Figure 4**), which was statistically significant in multivariable analysis, controlling for stage, histological subtype and age (**Table 3**).

Discussion

Gene expression regulation by promoter methylation is a well described epigenetic mechanism and its deregulation is considered an early event in carcinogenesis [36]. Indeed, aberrant promoter hypermethylation is associated with transcriptional repression [36, 37] and, thus, gene re-expression after demethylating treatment has been widely used as a strategy for identification of genes regulated by promoter methylation, namely in RCC [38-42]. *MST1R* promoter had been previously reported as hypermethylated in RCC in an area downstream of TSS [26, 27] and in the regions investigated by Angeloni and co-workers [22], but its putative association with altered *MST1R* expression pattern was not further explored. Our findings suggest that *MST1R* global expression ($MST1R_{total}$) is predominantly modulated by promoter methylation near TSS ($MST1R_{TSS}$), because significantly lower $MST1R_{total}$ expression was found in primary RCT with $MST1R_{TSS}$ hypermethylation, lower $MST1R_{total}$ expression was found in ccRCC cell lines with higher $MST1R_{TSS}$ methylation levels (769-P and 786-0), and $MST1R_{total}$ increased expression was observed in those cell lines after demethylating treatment.

It has been previously suggested that the pattern of promoter methylation was associated with the expression of different *MST1R* variants, specifically that the methylation of a particular promoter region upstream TSS - 'island 1' - was associated with lack of $flRON/MST1R_{long}$ and an increase of *sfRON* transcription, through an alternative internal promoter, with a consequent decrease in $MST1R_{long/total}$ ratio [22]. By bisulfite sequencing we found that not only the region previously described as 'island 1' but also its' upstream region within the CpG island were not methylated in RCTs, and thus we designed primers slightly upstream 'island 1' to further explore this *MST1R* promoter area. The quantification of *sfRON* expression could provide additional information concerning the variation of expression of different transcripts, but this was not possible due to the inability to design primers specific for *sfRON*. Surprisingly, a higher $MST1R_{long/total}$ ratio was found in RCTs with $MST1R_{up}$ hypermethylation (using a QMSP primer set specific to 'island 1'), although it did not reach statistical significance.

Because $MST1R_{long}$ is under control of the classical *MST1R* promoter, we hypothesized that transcription factors acting on *MST1R* in cancer cells might contribute to $MST1R_{long}$ expres-

sion, overcoming the methylation inhibitory effect. Since *NF-κB* has more predicted binding sites in the MST1R promoter than *HIF-1α* and *Egr-1*, *NF-κB* expression was determined in RCTs and, indeed, we found that RCTs with $MST1R_{up}$ hypermethylation displayed a significantly higher level of *NF-κB* expression, suggesting that promoter methylation is not the sole mechanism regulating *MST1R* expression.

Nevertheless, aberrant promoter methylation seems to be a relevant cause of *MST1R* silencing, because in 769-P and 786-O cells the $MST1R_{long/total}$ ratio increased after demethylating treatment. Importantly, increase in *flRON* expression after demethylating treatment had already been reported for other cell lines, including TF1 (erythroleukemia) and lung cancer cell lines [22].

We have previously reported that promoter methylation in a region downstream $MST1R_{TSS}$ identifies ccRCC with high sensitivity and specificity [26]. Similar diagnostic performance was not demonstrated for methylation of $MST1R_{up}$ or $MST1R_{TSS}$, neither for $MST1R_{total}$ expression or $MST1R_{long/total}$ ratio. Nevertheless, the present study demonstrated that lower $MST1R_{total}$ expression and higher $MST1R_{long/total}$ ratio independently predict worse prognosis in ccRCC and pRCC. Intriguingly, in urothelial carcinoma of the bladder, MST1R protein expression was associated with a worse prognosis [18] and *MST1R* overexpression is one of the mechanisms for activation of *MST1R* signaling, which seems to confer a more aggressive phenotype to cancer cells. However, it should be taken in account that in our series, *MST1R* overexpression is not a common alteration driving activation of signaling pathways that lead to cancer cell proliferation, invasion and metastization in RCC. On the contrary, we found significantly lower $MST1R_{total}$ expression in association with $MST1R_{TSS}$ hypermethylation in RCTs. Indeed, this contrasts with the more prominent role of *MST1R* in other cancer models, including nasopharyngeal carcinoma (NPC), in which latent membrane protein 1 (LMP1) stimulates NF-κB binding to *MST1R* promoter, inducing EMT, a finding that may explain the higher metastatic potential of NPC with LMP1 overexpression [19].

It should, however, be noted that the biological interpretation of *MST1R* expression in RCT primary tumor is not straightforward. We explored the association of *MST1R* promoter methylation pattern and $MST1R_{long/total}$ ratio, and given that *sfRON* is a constitutively active variant with oncogenic potential, it would be expectable that most aggressive tumors should display a lower $MST1R_{long/total}$ ratio. However, some $MST1R_{long}$ splicing variants have oncogenic potential, and even the overexpression of *MST1R* could lead to the activation of cell signaling pathways related to proliferation and metastization. The presence of such splicing variants, although functionally relevant for the understanding of *MST1R* role in renal carcinogenesis, was not further explored mainly because all are transcribed from the classical promoter and the $MST1R_{long}$ primer set was unable to discriminate splicing variants. Other *MST1R* activating mechanisms might also be relevant but their relative contribution might be limited. Indeed, the frequency of activating point mutations for RCC reported in COSMIC dataset (cancer.sanger.ac.uk) is low (3/1474, 0.2%), and the same holds true for the frequency of copy number variations (loss in 8/417, 1.9%) [27].

In conclusion, although promoter methylation patterns seem to determine *MST1R* global transcription regulation in renal cell carcinoma, other mechanisms might contribute to deregulate *MST1R* variant expression in RCT. Nevertheless, $MST1R_{total}$ expression and $MST1R_{long}$/$MST1R_{total}$ ratio modulate the biological and clinical aggressiveness of renal cell carcinoma, as depicted by its prognostic significance, a finding that requires validation in a larger independent series.

Acknowledgements

This study was funded by research grants from Research Center of Portuguese Oncology Institute of Porto (CI-IPOP 4-2012) and from Associação Portuguesa de Urologia (APU). ASP-L, JRC and IG are supported by FCT-Fundação para a Ciência e a Tecnologia fellowships (SFRH/SINTD/94217/2013, SFRH/BD/71293/2010 and CI-IPOP-BPD/UID/DTP/00776/2013, respectively).

Disclosure of conflict of interest

None.

Address correspondence to: Dr. Carmen Jerónimo, Portuguese Oncology Institute of Porto, Research Center-LAB 3, F Bdg., 1st floor, Rua Dr António Bernardino de Almeida, 4200-072 Porto, Portugal.

Tel: +351 225084000; Fax: +351 225084199; E-mail: carmenjeronimo@ipoporto.min-saude.pt; cljeronimo@icbas.up.pt

References

[1] Ronsin C, Muscatelli F, Mattei MG and Breathnach R. A novel putative receptor protein tyrosine kinase of the met family. Oncogene 1993; 8: 1195-1202.

[2] Gaudino G, Follenzi A, Naldini L, Collesi C, Santoro M, Gallo KA, Godowski PJ and Comoglio PM. RON is a heterodimeric tyrosine kinase receptor activated by the HGF homologue MSP. EMBO J 1994; 13: 3524-3532.

[3] Yoshimura T, Yuhki N, Wang MH, Skeel A and Leonard EJ. Cloning, sequencing, and expression of human macrophage stimulating protein (MSP, MST1) confirms MSP as a member of the family of kringle proteins and locates the MSP gene on chromosome 3. J Biol Chem 1993; 268: 15461-15468.

[4] Wang MH, Zhang R, Zhou YQ and Yao HP. Pathogenesis of RON receptor tyrosine kinase in cancer cells: activation mechanism, functional crosstalk, and signaling addiction. J Biomed Res 2013; 27: 345-356.

[5] Wang MH, Dlugosz AA, Sun Y, Suda T, Skeel A and Leonard EJ. Macrophage-stimulating protein induces proliferation and migration of murine keratinocytes. Exp Cell Res 1996; 226: 39-46.

[6] Cote M, Miller AD and Liu SL. Human RON receptor tyrosine kinase induces complete epithelial-to-mesenchymal transition but causes cellular senescence. Biochem Biophys Res Commun 2007; 360: 219-225.

[7] McClaine RJ, Marshall AM, Wagh PK and Waltz SE. Ron receptor tyrosine kinase activation confers resistance to tamoxifen in breast cancer cell lines. Neoplasia 2010; 12: 650-658.

[8] Gaudino G, Avantaggiato V, Follenzi A, Acampora D, Simeone A and Comoglio PM. The proto-oncogene RON is involved in development of epithelial, bone and neuro-endocrine tissues. Oncogene 1995; 11: 2627-2637.

[9] Wang MH, Wang D and Chen YQ. Oncogenic and invasive potentials of human macrophage-stimulating protein receptor, the RON receptor tyrosine kinase. Carcinogenesis 2003; 24: 1291-1300.

[10] Danilkovitch A and Leonard EJ. Kinases involved in MSP/RON signaling. J Leukoc Biol 1999; 65: 345-348.

[11] Danilkovitch A, Donley S, Skeel A and Leonard EJ. Two independent signaling pathways mediate the antiapoptotic action of macrophage-stimulating protein on epithelial cells. Mol Cell Biol 2000; 20: 2218-2227.

[12] Angeloni D, Danilkovitch-Miagkova A, Ivanov SV, Breathnach R, Johnson BE, Leonard EJ and Lerman MI. Gene structure of the human receptor tyrosine kinase RON and mutation analysis in lung cancer samples. Genes Chromosomes Cancer 2000; 29: 147-156.

[13] Maggiora P, Marchio S, Stella MC, Giai M, Belfiore A, De Bortoli M, Di Renzo MF, Costantino A, Sismondi P and Comoglio PM. Overexpression of the RON gene in human breast carcinoma. Oncogene 1998; 16: 2927-2933.

[14] Willett CG, Wang MH, Emanuel RL, Graham SA, Smith DI, Shridhar V, Sugarbaker DJ and Sunday ME. Macrophage-stimulating protein and its receptor in non-small-cell lung tumors: induction of receptor tyrosine phosphorylation and cell migration. Am J Respir Cell Mol Biol 1998; 18: 489-496.

[15] Chen Q, Seol DW, Carr B and Zarnegar R. Co-expression and regulation of Met and Ron proto-oncogenes in human hepatocellular carcinoma tissues and cell lines. Hepatology 1997; 26: 59-66.

[16] Maggiora P, Lorenzato A, Fracchioli S, Costa B, Castagnaro M, Arisio R, Katsaros D, Massobrio M, Comoglio PM and Flavia Di Renzo M. The RON and MET oncogenes are co-expressed in human ovarian carcinomas and cooperate in activating invasiveness. Exp Cell Res 2003; 288: 382-389.

[17] Chen WS, Kung HJ, Yang WK and Lin W. Comparative tyrosine-kinase profiles in colorectal cancers: enhanced arg expression in carcinoma as compared with adenoma and normal mucosa. Int J Cancer 1999; 83: 579-584.

[18] Cheng HL, Liu HS, Lin YJ, Chen HH, Hsu PY, Chang TY, Ho CL, Tzai TS and Chow NH. Co-expression of RON and MET is a prognostic indicator for patients with transitional-cell carcinoma of the bladder. Br J Cancer 2005; 92: 1906-1914.

[19] Chou YC, Chen CL, Yeh TH, Lin SJ, Chen MR, Doong SL, Lu J and Tsai CH. Involvement of recepteur d'origine nantais receptor tyrosine kinase in Epstein-Barr virus-associated nasopharyngeal carcinoma and its metastasis. Am J Pathol 2012; 181: 1773-1781.

[20] Yao HP, Zhou YQ, Zhang R and Wang MH. MSP-RON signalling in cancer: pathogenesis and therapeutic potential. Nat Rev Cancer 2013; 13: 466-481.

[21] Lu Y, Yao HP and Wang MH. Multiple variants of the RON receptor tyrosine kinase: biochemical properties, tumorigenic activities, and potential drug targets. Cancer Lett 2007; 257: 157-164.

[22] Angeloni D, Danilkovitch-Miagkova A, Ivanova T, Braga E, Zabarovsky E and Lerman MI. Hypermethylation of Ron proximal promoter as-

sociates with lack of full-length Ron and transcription of oncogenic short-Ron from an internal promoter. Oncogene 2007; 26: 4499-4512.
[23] Bardella C, Costa B, Maggiora P, Patane S, Olivero M, Ranzani GN, De Bortoli M, Comoglio PM and Di Renzo MF. Truncated RON tyrosine kinase drives tumor cell progression and abrogates cell-cell adhesion through E-cadherin transcriptional repression. Cancer Res 2004; 64: 5154-5161.
[24] Thangasamy A, Rogge J and Ammanamanchi S. Recepteur d'origine nantais tyrosine kinase is a direct target of hypoxia-inducible factor-1alpha-mediated invasion of breast carcinoma cells. J Biol Chem 2009; 284: 14001-14010.
[25] Xia Y, Lian S, Khoi PN, Yoon HJ, Han JY, Chay KO, Kim KK and Jung YD. Chrysin inhibits cell invasion by inhibition of Recepteur d'origine Nantais via suppressing early growth response-1 and NF-kappaB transcription factor activities in gastric cancer cells. Int J Oncol 2015; 46: 1835-1843.
[26] Pires-Luis ASL F, Vieira-Coimbra M, Costa-Pinheiro P, Antunes L, Oliveira J, Henrique R, Jerónimo C. MST1R methylation as a diagnostic biomarker in renal cell tumors. Acta Urológica Portuguesa 2015; 32: 64-70.
[27] Forbes SA, Beare D, Gunasekaran P, Leung K, Bindal N, Boutselakis H, Ding M, Bamford S, Cole C, Ward S, Kok CY, Jia M, De T, Teague JW, Stratton MR, McDermott U and Campbell PJ. COSMIC: exploring the world's knowledge of somatic mutations in human cancer. Nucleic Acids Res 2015; 43: D805-811.
[28] Moch H. An overview of renal cell cancer: pathology and genetics. Semin Cancer Biol 2013; 23: 3-9.
[29] Eble J SG, Epstein J, Sesterhenn I. Tumours of the kidney. In: J E, editors. WHO classification of tumours. Tumours of the urinary system and male genital organs. Lyon: IARC Press; 2004. p.
[30] Patton KT, Tretiakova MS, Yao JL, Papavero V, Huo L, Adley BP, Wu G, Huang J, Pins MR, Teh BT and Yang XJ. Expression of RON Proto-oncogene in Renal Oncocytoma and Chromophobe Renal Cell Carcinoma. Am J Surg Pathol 2004; 28: 1045-1050.
[31] Wang HY and Mills SE. KIT and RCC are useful in distinguishing chromophobe renal cell carcinoma from the granular variant of clear cell renal cell carcinoma. Am J Surg Pathol 2005; 29: 640-646.
[32] Edge SB BD, Compton CC, Fritz AG, Greene FL, Trotti A. AJCC Cancer Staging Manual. New York: Springer, 2010.
[33] Patricio P, Ramalho-Carvalho J, Costa-Pinheiro P, Almeida M, Barros-Silva JD, Vieira J, Dias PC, Lobo F, Oliveira J, Teixeira MR, Henrique R and Jeronimo C. Deregulation of PAX2 expression in renal cell tumours: mechanisms and potential use in differential diagnosis. J Cell Mol Med 2013; 17: 1048-1058.
[34] Pires-Luis AS, Vieira-Coimbra M, Vieira FQ, Costa-Pinheiro P, Silva-Santos R, Dias PC, Antunes L, Lobo F, Oliveira J, Goncalves CS, Costa BM, Henrique R and Jeronimo C. Expression of histone methyltransferases as novel biomarkers for renal cell tumor diagnosis and prognostication. Epigenetics 2015; 10: 1033-43.
[35] Costa VL, Henrique R, Danielsen SA, Duarte-Pereira S, Eknaes M, Skotheim RI, Rodrigues A, Magalhaes JS, Oliveira J, Lothe RA, Teixeira MR, Jeronimo C and Lind GE. Three epigenetic biomarkers, GDF15, TMEFF2, and VIM, accurately predict bladder cancer from DNA-based analyses of urine samples. Clin Cancer Res 2010; 16: 5842-5851.
[36] Feinberg AP, Ohlsson R and Henikoff S. The epigenetic progenitor origin of human cancer. Nat Rev Genet 2006; 7: 21-33.
[37] Sharma S, Kelly TK and Jones PA. Epigenetics in cancer. Carcinogenesis 2010; 31: 27-36.
[38] Ibanez de Caceres I, Dulaimi E, Hoffman AM, Al-Saleem T, Uzzo RG and Cairns P. Identification of novel target genes by an epigenetic reactivation screen of renal cancer. Cancer Res 2006; 66: 5021-5028.
[39] Kagara I, Enokida H, Kawakami K, Matsuda R, Toki K, Nishimura H, Chiyomaru T, Tatarano S, Itesako T, Kawamoto K, Nishiyama K, Seki N and Nakagawa M. CpG hypermethylation of the UCHL1 gene promoter is associated with pathogenesis and poor prognosis in renal cell carcinoma. J Urol 2008; 180: 343-351.
[40] Morris MR, Gentle D, Abdulrahman M, Maina EN, Gupta K, Banks RE, Wiesener MS, Kishida T, Yao M, Teh B, Latif F and Maher ER. Tumor suppressor activity and epigenetic inactivation of hepatocyte growth factor activator inhibitor type 2/SPINT2 in papillary and clear cell renal cell carcinoma. Cancer Res 2005; 65: 4598-4606.
[41] Morris MR, Gentle D, Abdulrahman M, Clarke N, Brown M, Kishida T, Yao M, Teh BT, Latif F and Maher ER. Functional epigenomics approach to identify methylated candidate tumour suppressor genes in renal cell carcinoma. Br J Cancer 2008; 98: 496-501.
[42] Morris MR, Ricketts C, Gentle D, Abdulrahman M, Clarke N, Brown M, Kishida T, Yao M, Latif F and Maher ER. Identification of candidate tumour suppressor genes frequently methylated in renal cell carcinoma. Oncogene 2010; 29: 2104-2117.